Pulse-Echo Field Distribution Measurement Technique for High-Frequency Ultrasound Sources

Kay Raum and William D. O'Brien, Jr., *Fellow, IEEE*

***Abstract*—A simple technique for the determination of the spatial and temporal transmit-receive field distributions of spherically focused high-frequency transducers is described. Instead of a point-like target, tungsten wires (line-like targets) with diameters less than the acoustic wavelength are used as pulse-echo targets. Spatial and temporal field quantities were determined for spherically focused transducers in the frequency range from 3 to 17 MHz, and a comparison with hydrophone measurements showed that both techniques yielded comparable results for the low-frequency transducer. However, for the higher frequency transducers, hydrophone measurements did not yield satisfactory results compared to the wire-target technique due to the hydrophone's aperture size, while the results from the wire-target technique were in general agreement with theory.**

I. Introduction

The use of spherically focused, high-frequency transducers is widespread in many high-resolution ultrasonic imaging applications such as in medical diagnosis and material investigations. The transducer itself is one of the most important components of an acoustic imaging system and knowledge about its transmit-receive spatial and temporal acoustic field characteristics is of fundamental interest for image generation and interpretation. A number of papers have been published on the prediction of transmitted pressure fields for arbitrary shaped and excited transducers. Most of the methods can be traced to the fundamental solutions of Rayleigh, King and Schoch [1], and one of the most powerful approaches was developed by Tupholme [2] and Stephanishen [3], [4]. Several techniques have been developed or evaluated for the measurement of transmit spatial field quantities such as the Schlieren technique [5], [6] where the interference of coherent light with the acoustic wave is used to project the spatial field distribution into a plane parallel to the acoustic beam axis, or for transmit spatial and temporal field quantities such as the hydrophone technique [7] where a three-dimensional field distribution and the instantaneous acoustic pressure can be obtained. Both techniques have significant disadvantages for the investigation of focused high-frequency transducers. The Schlieren method is limited to relatively low frequencies, up to about 15 MHz to date [6], due to the finite duration of the light pulse, and it requires an optical system which is not often available in acoustic laboratories. The use of a hydrophone is limited to relatively large acoustic beam dimensions due to its element size. Additionally, even though these techniques are able to predict and/or quantify acoustic field quantities, they do not take into account the transmit-receive behavior of the transducer on receive and the receive electronics.

A common technique to measure the pulse-echo temporal and spatial acoustic field distributions is to scan a small spherical shaped target across the acoustic beam [8]. However, this technique is limited when the beam cross-sectional area becomes comparable to the dimension of the target, particularly at higher frequencies. A target larger than the acoustic wavelength generally has to be used in order to obtain a satisfactory echo amplitude. Besides, the production of a small (point-like) target with the desired shape is difficult to realize. Another drawback is the time-intensive measurement procedure should a two-dimensional or three-dimensional field distribution be required.

In this contribution a simpler technique is described to obtain the projection of the spatial and temporal acoustic pressure distributions for high-frequency transducers. A small-diameter tungsten wire is used for the pulse-echo target. The scattering of an incident wave on a small cylinder is described in several papers [9]. The transmit-receive behavior and a CT reconstruction method using a small-diameter wire as a pulse-echo target at the focal plane has been described [10] wherein, for a CT reconstruction of the acoustic field, the wire was rotated within the focal plane, whereas, in the current investigation, a translational scan direction yielding a projection of the transmit-receive field distribution is being proposed.

Using a small-diameter wire instead of a point-like target enables one to choose a target size (wire diameter) smaller than the acoustic wavelength, even for higher frequencies. This provides good spatial (in axial and lateral scan direction) and temporal resolutions, while the received pressure amplitude is still sufficient due to the larger target area which is oriented perpendicular to the lateral scan direction and the beam axis. Additionally, as long as an axisymmetric field distribution can be assumed, only

Manuscript received June 3, 1996; accepted January 13, 1997. This work was supported in part by the Value-Added Research Opportunities Program, Agricultural Experiment Station, University of Illinois.

K. Raum is with Institute of Medical Physics and Biophysics, Martin-Luther-University Halle-Wittenberg, D-06097 Halle/Saale, Germany.

W. D. O'Brien is with Bioacoustics Research Laboratory, Department of Electrical and Computer Engineering, University of Illinois, Urbana, IL 61801 (e-mail: wdo@uiuc.edu).

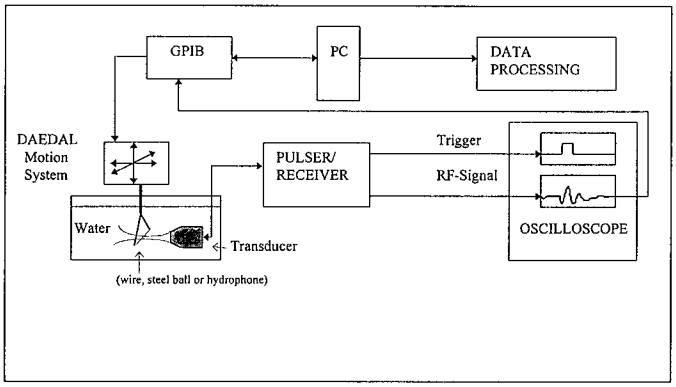

Fig. 1. Block diagram of the main system components.

two scan directions are necessary for a spatial field projection.

II. Methodology and Definitions

Fig. 1 is a block diagram showing the main components of the measurement system. The wire was placed in a tank filled with distilled, degassed water ($\approx 20°$C) and oriented normal to the sound beam direction. Tungsten wire targets with different diameters (25, 37, 63, 80 μm; California Fine Wire Company, Grover City, CA) were used. For comparison, a 3.175-mm diameter stainless steel ball was also used as a target. The transmitted field distribution was measured with a calibrated PVDF bilaminar membrane hydrophone with an effective diameter of 0.785 ± 0.007 mm (Model 804, Sonic Industries, Hatboro, PA). Spherically focused transducers with nominal center frequencies of 15 and 20 MHz (Panametrics V319 and V317, respectively; Waltham, MA) and, for comparison, a weakly focused 3-MHz transducer (Panametrics V3680) were used. The transducers were excited by a 300 V mono-cycle pulse produced by a computer-controlled pulser/receiver (Model 5800; Panametrics, Waltham, MA). For the transmit-receive measurements, the receive signal was amplified (20 dB) and band-pass filtered (1-35 MHz) by the pulser/receiver. For all measurements, the signal was displayed (500 Ms/s) on a digitizing oscilloscope (Model 11401; Tektronix) with a 10-bit resolution. Either the targets or the hydrophone were scanned across the acoustic field using a computer-controlled micro-precision positioning system (Daedal Inc., Harrison City, PA) with positional accuracy of about 2 μm. The grid size spacings in the lateral and axial directions were 25 μm and 50 μm for the wire measurements, respectively, and 50 μm in both lateral directions for the steel ball and hydrophone measurements. The positioning system, oscilloscope, and pulser/receiver were connected to a GPIB board and controlled by a 486-66 PC. The time window at the oscilloscope was moved with every axial scan movement to maintain a high sampling rate (500 Ms/s) with a low number of sample points. Each 512-point A-scan was stored to the PC hard drive and transferred to a SUN Sparc 20 workstation for off-line processing. All computations were performed with MATLAB® (The MathWorks, Inc., Natick, MA).

The lateral acoustic pressure distribution in the focal plane of a spherical focusing source is described by [11], [12]:

$$\left|\frac{p(r)}{p(0)}\right| = \left|\frac{2J_1\left(\frac{kar}{\mathrm{ROC}}\right)}{\frac{kar}{\mathrm{ROC}}}\right| \tag{1}$$

where $p(r)$ is the peak acoustic pressure as a function of the off-axis lateral distance r, $p(0)$ is the on-axis peak acoustic pressure at $z = \mathrm{ROC}$, k is the wave number, a is the radius of the transducer and ROC is the transducer's radius of curvature where ROC is also considered the focal length at the geometrical focus; the true focus (maximum axial intensity location) is located closer to the transducer ($z <$ ROC) due to diffraction effects. $J_1(x)$ is the Bessel function of the first kind of order one. From (1) the -3-dB transmit and -6-dB transmit-receive beam width (diameter) in the geometrical focal plane ($z = \mathrm{ROC}$) (also the definition used herein for the lateral resolution) is:

$$D_{\mathrm{lateral}} = 1.028 \cdot \lambda \cdot f^{\#} \tag{2}$$

where $f^{\#}$ is the *f-number* ($= \mathrm{ROC}/2a$) and λ is the acoustic wavelength.

The axial acoustic pressure distribution of a spherical focusing source is described by [11], [12]:

$$\left|\frac{p(z)}{p(0)}\right| = \frac{\mathrm{ROC}}{z}\left|\mathrm{sinc}\left(\frac{a^2}{2\lambda \mathrm{ROC}}\left(\frac{\mathrm{ROC}}{z} - 1\right)\right)\right| \tag{3}$$

where $p(z)$ is the peak acoustic pressure as a function of the axial distance z, and the $\mathrm{sinc}(x)$ function is $\frac{\sin(\pi x)}{\pi x}$. From (3) the approximate -3-dB transmit and -6-dB transmit-receive depth of focus (also the definition used herein for the depth of focus) is:

$$F_z = 7.08 \cdot \lambda \cdot f^{\#^2}. \tag{4}$$

For a pulse-echo wire target, the line integral of the acoustic pressure projection $f_p(x, z)$ is obtained instead of the point-to-point pressure distribution, that is,

$$f_p(x, z) = \int p(x, y, z)dy \tag{5}$$

where the wire is parallel to the y axis. While a theoretical evaluation is beyond the scope of this contribution, the geometry dictates that the beam must be symmetric about the beam axis and have relatively weak side lobes in order to properly characterize the field's dimensions near the beam axis. These conditions are satisfied for strongly focused beams from a spherical transducer.

All acoustic field definitions were based on the *Acoustic Output Measurement and Labeling Standard for Diagnostic Ultrasound Equipment* [13]. Spatial field distributions were determined from the spatial distribution of the

pulse intensity integral (*PII*) which is the time integral of the instantaneous intensity for any specific point and pulse integrated over the time in which the envelope of acoustic pressure (total pressure minus ambient pressure) is nonzero. The focal length at the true focus (F), depth of focus (F_z) and beam width at the true focal plane (D_{lateral}) were determined from a spatial map of the normalized *PII*. The focal length is the distance along the beam axis from the transducer surface to the true focal plane, that is, the location where the *PII* value is a maximum.

The propagation speed was determined from the slope of the on-axis time-of-flight of the received maximum acoustic pressure amplitude versus the axial position z of the wire target, that is,

$$c = \frac{2\Delta z}{\Delta t}. \tag{6}$$

The pulse duration (τ), bandwidth (Δf), center frequency (f_c) and fractional bandwidth were determined from the RF-signal at the true focal point. The pulse duration ($\tau_{(10\text{–}90\%)}$) is 1.25 times the interval between the time when the time integral of intensity in an acoustic pulse at a point reaches 10 percent and when it reaches 90 percent of the *PII* value [13]. Alternately, and also used herein, the pulse duration ($\tau_{(-20\text{ dB})}$) is defined as the time duration between the times when the pulse amplitude is at −20 dB of its maximum values. From the spatial extent of the pulse duration, the axial resolution is determined from:

$$D_{\text{axial}} = \frac{c \cdot \tau}{2}. \tag{7}$$

The bandwidth Δf is the difference in the frequencies f_1 and f_2 at which the acoustic pressure spectrum is −3 dB of its maximum value, the center frequency is $f_c = (f_1 + f_2)/2$ and the fractional bandwidth is the bandwidth divided by the center frequency and expressed as a percentage.

III. Results and Discussion

Transmit-receive spectral characteristics of the three transducers used to evaluate the measurement technique yielded center frequencies at slight variance with the manufacturer's stated center frequencies. For consistency in the following discussion, the three transducers are referred to by the manufacturer's stated center frequencies of 3, 15, and 20 MHz.

The measured propagation speed in distilled, degassed water varied between 1482 and 1495 m/s at a temperature of about 19.5°C, whereas the actual propagation speed at 20°C is 1482.7 m/s [14]. Thus, using (6) may provide a technique for propagation speed determination simultaneously with field measurements although, for the calculations reported herein, a propagation speed of 1482 m/s was used.

The optimal wire diameter was assessed by evaluating the −6-dB transmit-receive beam width in the true focal plane as a function of different wire sizes (25 to 80 μm) for the three transducers (Table I). The 3-MHz transducer wavelength (412 μm) and measured beam width ($\approx$ 2250 μm) were much larger than the wire diameters and, as expected, the various wire diameter sizes did not have an appreciable effect on the measured beam width (mean agreement to within 6.8%). Likewise, the hydrophone-determined −3-dB transmit beam width and the wire-determined −6-dB transmit-receive beam width were comparable for the 3-MHz transducer field. For the 15- and 20-MHz transducer fields with wavelengths of 114 and 86 μm, the wire diameter did not have an appreciable effect on the measured beam widths (mean agreements to within 6.6 and 2.9%, respectively) whereas the hydrophone-determined and steel ball-determined beam widths were considerably greater. The calculated lateral beam widths [from (2)] for the 3-, 15-, and 20-MHz transducers were 2117, 175, and 176 μm, respectively, compared to the four wire-determined lateral beam-width ranges of 2210–2365, 175–187, and 173–178 μm, and therefore, the experimental observations support the suggestion that a wire diameter less than the acoustic wavelength is sufficient to obtain the correct field dimensions for spherically focused fields.

Pulse duration, bandwidth and center frequency were obtained from the true focal point RF signal using a 25-μm wire (Fig. 2). Significantly different values for the pulse duration were obtained using the different definitions, each of which also yielded different calculated values for the axial resolution (Table II). Also, the hydrophone-determined (transmit) pulse duration (either definition) was significantly smaller than the transmit-receive pulse duration, that is, $\tau_{(10\text{–}90\%)}$ is 75 ns (hydrophone) versus 135 ns (wire) for the 15-MHz transducer and 50 ns (hydrophone) versus 84 ns (wire) for the 20-MHz transducer, and $\tau_{(-20\ dB)}$ is 175 ns (hydrophone) versus 250 ns (wire) for the 15-MHz transducer and 110 ns (hydrophone) versus 155 ns (wire) for the 20-MHz transducer.

The manufacturer's transducer certification documents provided selected field values from transmit-receive measurements using a 3.3-mm diameter steel ball target. Our spectral measurements with a 3.175-mm-diameter stainless steel ball target were generally not in agreement with the manufacturer's results wherein the high-frequency transducers varied significantly from the manufacturer's descriptions (Table II). It was found that the 35-MHz pulser/receiver used in this study appeared to attenuate the higher frequency components which resulted in the estimated center frequencies of the two higher frequency probes being considerably lower than the manufacturer-stated frequencies, that is, 13.05 MHz for the 15-MHz transducer and 17.33 MHz for the 20-MHz transducer. Also, it was observed that the frequency spectra from the steel ball target contained more than one frequency peak, probably as a result of multipath propagation within the steel ball, thus suggesting that a steel ball may not be the best target for such measurements. However, the manu-

TABLE I

TRANSMIT-RECEIVE −6-DB BEAM WIDTHS AT THE TRUE FOCAL POINT WERE OBTAINED FROM FOUR DIFFERENT WIRE DIAMETERS, AND FROM ONE 3.175-MM-DIAMETER STAINLESS STEEL BALL. THE TRANSMIT −3-DB BEAM WIDTHS AT THE TRUE FOCAL POINT WERE OBTAINED FROM ONE 0.785-MM EFFECTIVE-DIAMETER HYDROPHONE. (BLANK INDICATES NO MEASUREMENT WAS MADE).

Target	V3680 3-MHz Transducer	V319 15-MHz Transducer	V317 20-MHz Transducer
25-μm wire	2250 μm	187 μm	173 μm
37-μm wire	2210 μm	181 μm	173 μm
63-μm wire	2215 μm	175 μm	176 μm
80-μm wire	2365 μm	187 μm	178 μm
Hydrophone	2305 μm	665 μm	760 μm
Stainless Steel Ball		495 μm	460 μm

TABLE II

MEASURED SPATIAL AND TEMPORAL FIELD QUANTITIES USING A 25-μM WIRE TARGET. WHERE APPLICABLE, COMPARISON OF MEASURED QUANTITIES WITH MANUFACTURER'S CERTIFICATION OR CALCULATED VALUES IS PROVIDED (CALCULATED VALUES ARE DENOTED WITH AN * AND A BLANK INDICATES EITHER THE INFORMATION WAS NOT MEASURED OR THE MANUFACTURER DID NOT PROVIDE THE INFORMATION).

	V3680 3-MHz Transducer		V319 15-MHz Transducer		V317 20-MHz Transducer	
Transducer or field quantity	Measured	Certification/ Calculated*	Measured	Certification/ Calculated*	Measured	Certification/ Calculated*
F		100 mm	18.70 mm	19.05 mm	12.44 mm	12.70 mm
a		10 mm		6.35 mm		3.175 mm
f-number		5		1.5		2
F_z		72.9 mm*	1.80 mm	1.81 mm*	2.15 mm	2.42 mm*
D_{lateral}	2.3 mm	2.1 mm*	187 μm	175 μm*	173 μm	176 μm*
f_1	2.70 MHz		11.05 MHz	10.60 MHz	13.65 MHz	15.80 MHz
f_2	4.45 MHz		15.05 MHz	19.80 MHz	21.00 MHz	27.70 MHz
f_c	3.60 MHz		13.05 MHz	15.20 MHz	17.33 MHz	21.75 MHz
Δ_f	1.75 MHz		4.00 MHz	9.20 MHz	7.35 MHz	5.95 MHz
Fractional Bandwidth	48.6%		30.7%	60.5%	42.4%	27.4%
$\tau_{(-20\text{ dB})}$	620 ns		250 ns	163 ns	155 ns	146 ns
$\tau_{(10\text{–}90\%)}$	375 ns		135 ns		84 ns	
D_{axial} (using $\tau_{(-20\text{ dB})}$)	460 μm		186 μm	121 μm*	115 μm	108 μm*
D_{axial} (using $\tau_{(10\text{–}90\%)}$)	278 μm		100 μm		63 μm	

facturer's focal length was slightly greater but in general agreement with measurements reported herein.

The two-dimensional hydrophone-determined (transmit only) contour lateral distributions were obtained from both the 3- and 20-MHz transducer fields in the true focal planes (Figs. 3(a) and 3(b), respectively), along with their respective one-dimensional lateral distributions (dashed lines in Figs. 3(c) and 3(d), respectively). The hydrophone's effective diameter (785 μm) is smaller than the 3-MHz transducer's lateral resolution (2.3 mm) by a factor of about 3 and is larger than the 20-MHz transducer's lateral resolution (173 μm) by a factor of about 4.5. This demonstrates that the hydrophone's effective diameter is dominant over that of the field's actual lateral distribution when the target size is larger than significant spatial changes of the field's pressure distribution.

The one-dimensional hydrophone-determined (transmit only) normalized lateral distributions in the true focal planes for the 3- and 20-MHz transducer fields were compared to the wire-determined (transmit/receive) normalized lateral distributions in the same planes [Figs. 3(c) and 3(d)]. The wire diameters were 80 and 25 μm for the 3- and 20-MHz transducer field distributions, respectively. The transmit and transmit-receive 3-MHz lateral field distributions appear to be essentially the same [Fig. 3(c)]; however, there are differences because the hydrophone-determined pressure amplitude distribution is a function of $\left|\frac{2J_1(x)}{x}\right|$ [see (1)] whereas, for the wire-determined distribution, $\left|\frac{2J_1(x)}{x}\right|^2$. This is observed for the distributions further away from the beam axis where the transmit-receive distribution (with wire target) exhibits a slightly steeper slope compared to that of the transmit distribution (with hydrophone). However, near the beam axis the hydrophone- and wire-determined distributions are almost equivalent, thus supporting the suggestion that for larger beam dimensions both techniques become comparable.

The hydrophone-determined (transmit only) and wire-determined (transmit-receive) 20-MHz lateral field distributions are quite different [Fig. 3(d)]. The transmit-receive field distribution obtained with the 25-μm wire is in good agreement with the theoretical calculation of the 20-MHz transducer's lateral distribution (Table II). This result is

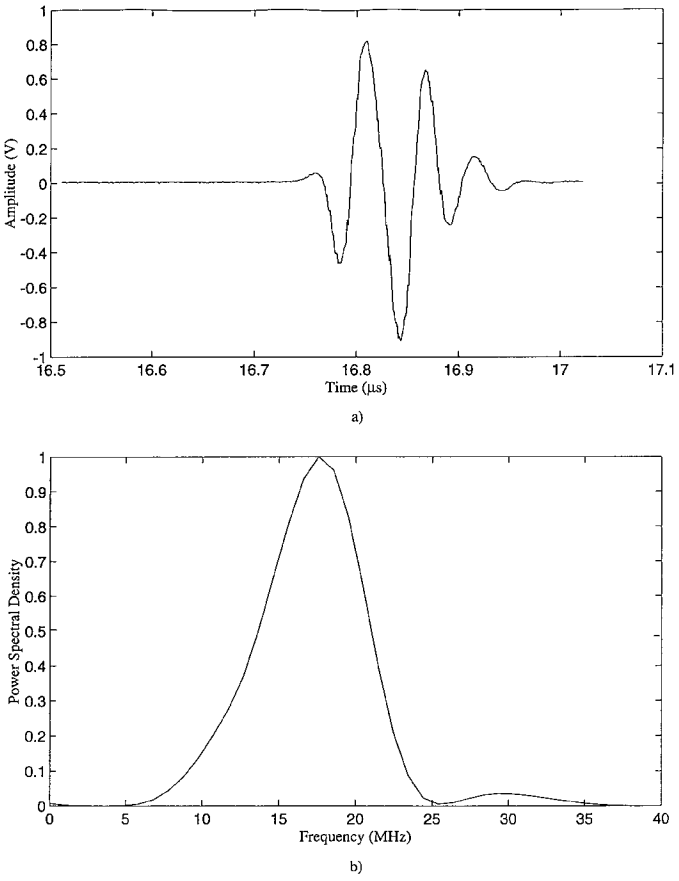

Fig. 2. (a) Pulse-echo response and (b) power density spectrum of the 20-MHz transducer field. A 25-μm wire target was positioned at the on-axis true focal location.

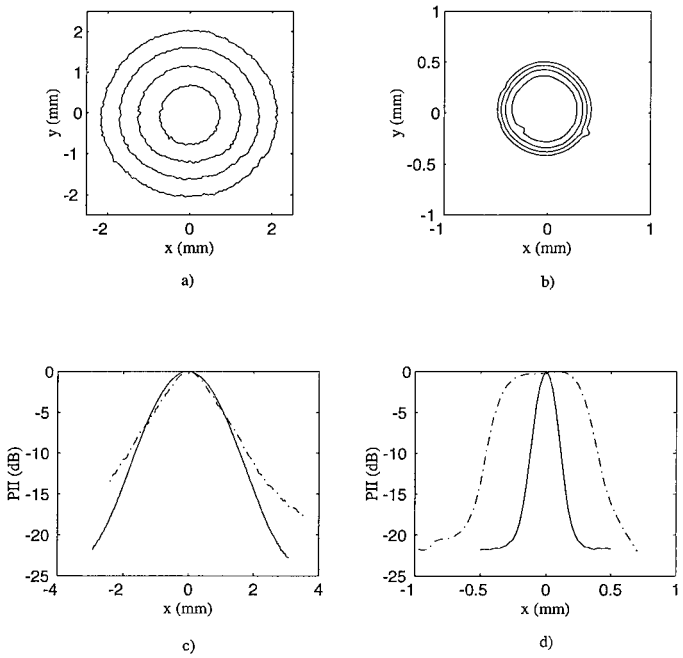

Fig. 3. Two-dimensional hydrophone-determined (transmit) lateral field contour distributions measured in the true focal plane where each contour line is separated by 3 dB for the (a) 3-MHz and (b) 20-MHz transducers. One-dimensional wire-determined (transmit-receive) lateral field distributions were measured in the true focal plane for the (c) 3-MHz transducer with an 80-μm-diameter wire and (d) 20-MHz transducer with a 25-μm-diameter wire (solid lines). Dashed lines in (c) and (d) correspond to the one-dimensional hydrophone-determined (transmit) lateral field distributions measured in the true focal plane.

reasonable, since the contribution to the observed line integral from scatterers located at a larger radial distance is greatly decreased due to the much weaker, side lobe off-axis intensity. Therefore, for a small lateral off-axis distance, the field distribution obtained using a small wire target can be assumed to be a point-to-point distribution.

Fig. 4 is a contour plot of the 20-MHz transducer field where each contour line represents a 3-dB decrease of the *PII* value. The true focal length was determined from the on-axis time-of-flight of the received signal at the maximum *PII* location. The measured focal length (F), depth of focus (F_z) and beam width (D_{lateral}) at the focal plane are comparable to the calculated theoretical values (Table II).

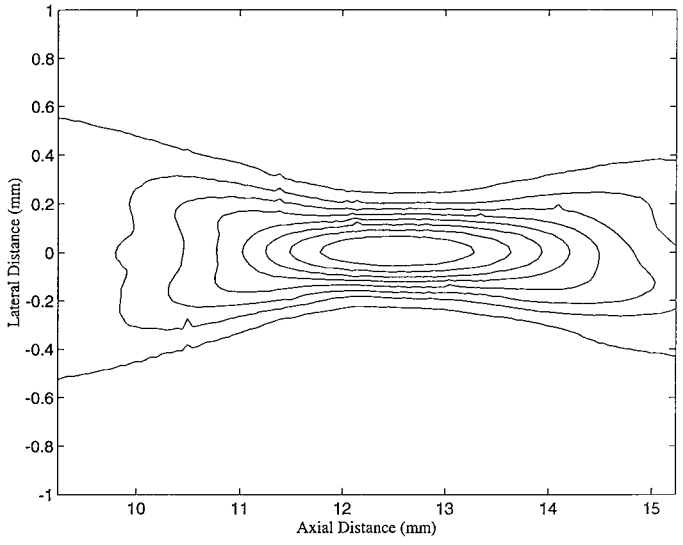

Fig. 4. Contour plot of the spatial intensity distribution (*PII* in dB) of the 20-MHz transducer field. Each contour line indicates a decrease of the *PII* value of 3 dB.

IV. Conclusion

The results demonstrate that the wire-target technique is a simple and powerful measurement procedure to determine the spatial and temporal transmit-receive acoustic field quantities from high-frequency sources when an appropriately small effective hydrophone diameter is not available. For the low-frequency case investigated herein, the hydrophone and wire-target techniques yielded comparable results. For the two high-frequency cases, the wire-

target technique yielded spatial field information more consistent with the calculated theoretical quantities. Also, from the wire-target reflected waveform from the focal point, appropriate temporal field quantities could be determined. In principal there are no upper frequency limits for the wire-target technique as long as the wire diameter is smaller than the acoustic wavelength and the signal-to-noise is adequate.

References

[1] G. R. Harris, "Review of transient field theory for a baffled planar piston," *J. Acoust. Soc. Amer.*, vol. 70, no. 1, pp. 10–20, 1981.

[2] G. E. Tupholme, "Generation of acoustic pulses by baffled plane pistons," *Mathematika*, vol. 16, pp. 209–224, 1969.

[3] P. R. Stephanishen, "The time-dependent force and radiation impedance on a piston in a rigid infinite planar baffle," *J. Acoust. Soc. Amer.*, vol. 49, no. 3, pp. 841–849, 1971.

[4] P. R. Stephanishen, "Transient radiation from pistons in a infinite planar baffle," *J. Acoust. Soc. Amer.*, vol. 49, no. 5, pp. 1629–1638, 1971.

[5] D. R. Newmann, "Ultrasonic Schlieren system using a pulsed gas laser," *IEEE Trans. Sonics Ultrason.*, vol. SU-20, pp. 282–285, July, 1973.

[6] B. Schneider and K. K. Shung, "Quantitative analysis of pulsed ultrasonic beam patterns using a Schlieren system," *IEEE Trans. Ultrason., Ferroelect., Freq. Contr.*, vol. 43, no. 6, pp. 1181–1186, 1996.

[7] D. R. Bacon, "Characteristics of a PVDF membrane hydrophone for use in the range 1–100 MHz," *IEEE Trans. Sonics Ultrason.*, vol. SU-29, pp. 18–25, 1982.

[8] C. A. Bernier, "A practical approach to measuring an intravascular ultrasonographic imaging system beam pattern," *J. Ultrasound Med.*, vol. 14, pp. 367–372, 1995.

[9] T. Li and M. Ueda, "Sound scattering of a plane wave obliquely incident on a cylinder," *J. Acoust. Soc. Amer.*, vol. 86, no. 6, pp. 2363–2368, 1989.

[10] T. Li, H. Shimamoto, and M. Ueda, "Measurement of transmit-receive sound intensity pattern of ultrasound transducer using echoes scattered by a fine wire," *J. Acoust. Soc. Jpn.*, vol. 46, no. 10, pp. 810–816, 1990.

[11] B. G. Lucas and T. G. Muir, "The field of a focusing source," *J. Acoust. Soc. Amer.*, vol. 72, no. 4, pp. 1289–1296, 1982.

[12] G. S. Kino, *Acoustic Waves: Devices, Imaging, and Analog Signal Processing*. Englewood Cliffs, NJ: Prentice-Hall, Inc., 1987.

[13] American Institute of Ultrasound in Medicine, *Acoustic Output Measurement and Labeling Standard for Diagnostic Ultrasound Equipment*. Laurel, MD: Amer. Inst. Ultrasound Med., 1992.

[14] W. L. Nyborg. *Intermediate Biophysical Mechanics*. Menlo Park, CA: Cummings Publishing Co., 1975.

Kay Raum was born in Halle/Saale, Germany, on March 1, 1972. He received his Vordiplom in Physics from the Martin Luther University of Halle-Wittenberg in 1993. From 1995–1996 he was with the Bioacoustics Research Laboratory at the University of Illinois at Urbana-Champaign as a Visiting Scholar. Currently he is pursuing his Diplom degree in Physics from the Martin Luther University of Halle-Wittenberg.

His interests are in high frequency acoustic imaging and characterization of biological tissues.

William D. O'Brien, Jr. (S'64–M'70–SM'79–F'89) received the B.S, M.S., and Ph.D. degrees in 1966, 1968, 1970, from the University of Illinois, Urbana-Champaign.

From 1971 to 1975 he worked with the Bureau of Radiological Health (currently the Center for Devices and Radiological Health) of the U.S. Food and Drug Administration. Since 1975, he has been at the University of Illinois, where he is a Professor of Electrical and Computer Engineering and of Bioengineering, College of Engineering, and Professor of Bioengineering, College of Medicine. He is the Director of the Bioacoustics Research Laboratory and the Program Director of the NIH Radiation Biophysics and Bioengineering in Oncology Training Program. His research interests involve the many areas of acoustics and ultrasound, including spectroscopy, risk-assessment, biological effects, tissue characterization, dosimetry, blood-flow measurements, acoustic microscopy, and imaging. He has published more than 180 papers.

Dr. O'Brien is Editor-in-Chief of the *IEEE Transactions on Ultrasonics, Ferroelectrics, and Frequency Control*. He is a Fellow of the Institute of Electrical and Electronics Engineers (IEEE), the Acoustical Society of America (ASA), and the American Institute of Ultrasound in Medicine (AIUM), and he is a Founding Fellow of American Institute of Medical and Biological Engineering. He was recipient of the IEEE Centennial Medal (1984), the AIUM Presidential Recognition Awards (1985 and 1992), the AIUM/WFUMB Pioneer Award (1988), the IEEE Outstanding Student Branch Counselor Award (1989), and the AIUM Joseph H. Holmes Basic Science Pioneer Award (1993). He has been President (1982–1983) of the IEEE Sonics and Ultrasonics Group (currently the IEEE UFFC Society), Co-Chairman of the 1981 IEEE Ultrasonic Symposium, and General Chairman of the 1988 IEEE Ultrasonics Symposium, President of the AIUM (1988–1991), and Treasurer of the World Federation for Ultrasound in Medicine and Biology (1991–1994). He is the 1997–1998 IEEE UFFC Society's Distinguished Lecturer.